DOCUMENT NO 73SD2180

AFCRL TR - 73 - 0671

ELECTRON DENSITY DISTRIBUTION OVER BLUNT

BODIES IN THREE DIMENSIONAL FLOW

by

Henry G. Lew

GENERAL ELECTRIC COMPANY
VALLEY FORGE, PENNSYLVANIA 19101

Contract No. F19628-72-C-0070
Project No. 4642
Task No. 464202
Work Unit No. 46420201

SCIENTIFIC REPORT NO. 2

OCTOBER 1973

Contract Monitor: John F. Lennon
Microwave Physics Laboratory

Approved for public release; distribution unlimited.

Prepared for

AIR FORCE CAMBRIDGE RESEARCH LABORATORIES
AIR FORCE SYSTEMS COMMAND
UNITED STATES AIR FORCE
BEDFORD, MASSACHUSETTS 01730

UNCLASSIFIED
Security Classification

DOCUMENT CONTROL DATA - R & D		
(Security classification of title, body of abstract and indexing annotation must be entered when the overall report is classified)		
1. ORIGINATING ACTIVITY (Corporate author) General Electric Company Re-entry & Environmental Systems Div. Valley Forge, Pennsylvania 19101	2a. REPORT SECURITY CLASSIFICATION Unclassified	
	2b. GROUP	

3. REPORT TITLE

ELECTRON DENSITY DISTRIBUTION OVER BLUNT
BODIES IN THREE DIMENSIONAL FLOW

4. DESCRIPTIVE NOTES (Type of report and inclusive dates)
Scientific -   - Interim

5. AUTHOR(S) (First name, middle initial, last name)

Henry G. Lew

6. REPORT DATE October 1973	7a. TOTAL NO. OF PAGES 54	7b. NO. OF REFS 25
8a. CONTRACT OR GRANT NO. F19628-72-C-0070 b. PROJECT, TASK, AND WORK UNIT NO. 4642-02-01 c. DOD ELEMENT 62101F d. DOD SUBELEMENT 684642	9a. ORIGINATOR'S REPORT NUMBER(S) GE TIS 73SD2180 Scientific Report No. 2	
	9b. OTHER REPORT NO(S) (Any other numbers that may be assigned this report) AFCRL TR - 73 - 0671	

10. DISTRIBUTION STATEMENT

A - Approved for public release; distribution unlimited.

11. SUPPLEMENTARY NOTES TECH, OTHER	12. SPONSORING MILITARY ACTIVITY Air Force Cambridge Research Laboratories (LZ) L. G. Hanscom Field Bedford, Massachusetts 01730

13. ABSTRACT

SUMMARY

The electron density distribution in the shock layer of re-entry bodies in hypersonic flight is determined by many factors. Among these, the effect of a nonzero angle-of-attack of the body to the free stream is an important one. This report considers the three dimensional boundary layer over a sphere-cone body at hypersonic flight and a nonzero angle-of-attack at conditions where the air is a mixture of dissociated and ionized components reacting with each other at finite chemical rates. The equations of motion for the three dimensional flow are formulated and method of attack by an implicit finite difference scheme is utilized for their solutions. Edge conditions with partial swallowing for the boundary layer are obtained directly from the inviscid equations of motion which are solved by an iterative finite difference predictor-corrector method. Finally, illustrative numerical results of the three dimensional flow effects are presented for flow over the AFCRL Trailblazer II Body.

DD FORM 1473
NOV 65

UNCLASSIFIED
Security Classification

KEY WORDS	LINK A		LINK B		LINK C	
	ROLE	WT	ROLE	WT	ROLE	WT
Ionized Flow, Viscous Shock Layer, Boundary Layer, Electron Density, Three Dimensional Blunt Body Flow Field.						

SUMMARY

The electron density distribution in the shock layer of re-entry bodies in hypersonic flight is determined by many factors. Among these, the effect of a nonzero angle-of-attack of the body to the free stream is an important one. This report considers the three dimensional boundary layer over a sphere-cone body at hypersonic flight and a nonzero angle-of-attack at conditions where the air is a mixture of dissociated and ionized components reacting with each other at finite chemical rates. The equations of motion for the three dimensional flow are formulated and a method of attack by an implicit finite difference scheme is utilized for their solutions. Edge conditions with partial swallowing for the boundary layer are obtained directly from the inviscid equations of motion which are solved by an iterative finite difference predictor-corrector method. Finally, illustrative numerical results of the three dimensional flow effects are presented for flow over the AFCRL Trailblazer II body.

TABLE OF CONTENT

I. Introduction

The production of electrons at hypersonic speeds in the shock layer
of a blunt body is a direct function of the conversion of kinetic energy
of flight to heat which is dependent principally on the aerodynamic flight
configuration. At the high temperatures created electrons are obtained
from the various energy exchanges in the hot dissociated air about the
body. The existence of a layer of electrons about re-entry body leads
to several detrimental effects; one of the principal effect is the attenua-
tion of electromagnetic signals propagating through the layer leading to
telemetry blackout. A number of studies has been made of this problem.
These studies have involved both flight measurements of the severity of
the problem [1], [2] and theoretical predictions of the degree of ioniza-
tion in the shock layer [3], [4], [5] with comparison of flight data with
theoretical results [1] [2]. Good agreement was found between theoretical
prediction and flight measurement of electron density about the Trailblazer
sphere-cone body at hypersonic speeds at applicable conditions.

The prediction of electron density about hypersonic re-entry vehicles
in the viscous region near the body was given in reference (3) and (4) for
the sphere cone body. Numerical results for the AFCRL Trailblazer II
vehicle at hypersonic speed were given. These results were made princi-
pally for bodies at zero angle-of-attack. Since the gaseous environment
is composed of hot dissociated species internal energy transfers become
important. The effect of energy distribution in the various energy modes,
in particular, the vibrational relaxation process may change the production
of electrons. A study of these effect and surface catalyticity on the

- 1 -

electron density distributions was considered in reference (5) with numerical results for the AFCRL Trailblazer vehicle.

Flight of the Trailblazer vehicle has shown that the angle-of-attack is of the magnitude of 10° to 15° with respect to the free stream. The asymmetry of the flow introduced by this flight angle lead to significant changes in the flow field characteristics of velocity, temperature, and concentration of the dissociated and ionized air species. The magnitude of the effect of the non-zero angle-of-attack is usually determined by the relative sizes of the angle-of-attack and the half-cone angle. If α is the angle-of-attack and θ_c the cone half-angle then small angle-of-attack effects are restricted to values of $(\alpha/\theta_c) < 1$. For the Trailblazer vehicle the cone angle is 9° so that $\alpha/\theta_c > 1$; that is, the effect of angle-of-attack is large. Observation of some of the effects of large angle-of-attack has been made. The pattern for flow over a blunt cone at non-zero angle-of-attack has been obtained from experiments. Laboratory experiments by Tracy[6] have shown that the viscous layer on the leeward side of a circular cone grows exponentially to the point of flow separation and subsequently alters the inviscid flow. Later experiments by Stetson in 1971 gave additional details. Stetson's measurement[7] indicate that there are formed symmetrical helical vortices with no reverse flow.

In general, the non-zero angle-of-attack generates two effects which are important to the distribution of electron density over a blunt conical body. First, the pressure is increased on the windward side. This increase can be large. Examples of this increase can be seen from Stetson's

experimental measurement [7] of the flow over a 5.6^o half-angle blunt

cone. For a bluntness ratio of 0.1 and for $X/R_N = 5$ (X is the wetted

length measured from the tip, R_N is the nose radius), the surface pres-

sure ratio on the most windward meridian plane has been increased by

a factor of 2 as the angle-of-attack is increased from zero to 10°.

The maximum Trailblazer vehicle X/R_N is 4.25 and its bluntness ratio

is 0.664 and its cone half-angle is 9°. Thus a factor of 2 to 3 in-

crease in pressure would be expected on the windward meridian plane.

This surface pressure distribution decreases in value as the flow

sweeps toward the leeward plane; at this latter plane the pressure drops

below the values at zero angle-of-attack. Thus the increase of pressure

will lead to a noticeable effect on the electron density by the increase

in production rate of electrons.

A second effect is the divergence of surface streamlines from the

inviscid streamlines. Rakich, et al [8] has made an oil-film experi-

ment of the surface streamlines showing the turning of the viscous

streamlines near the body relative to the inviscid streamlines as shown

on Figure 1.1. The significance of the cross flow can be appreciated by

reference to Figure 1.1 where the increasing divergence in the directions

of the boundary layer and inviscid flow streamlines downstream is shown.

The region of influence as noted in the Figure outlines the entire region

influenced by the original planar meridian streamlines. The curvature

of the fluid streamlines near the wall becomes much different from that

of the inviscid streamlines due to the cross flow generated by a non-

zero angle-of-attack. Species concentrations are changed locally by

convection following the increased divergency of streamlines.

The mathematical characteristics of the three dimensional boundary layer still remain parabolic. However, a large difference appears with the addition of the one coordinate. Characteristics such as momentum, energy, and species concentrations are diffused normal to the surface and convected by streamlines downstream into the zone of influence shown on Figure 1. 1. The electron concentration generated at the stagnation region spread over the windward side and then to leeward side of the cone. Thus the second effect of non-zero angle-of-attack is the divergency of the surface streamlines toward the leeward plane. This results in convection of electrons away from the windward planes. Consequently, one can say that the net effect of a non-zero angle-of-attack is to generate more electrons and to transport them out of the meridian plane to all other parts of the flow field.

This report is concerned with the continuation of the previous studies[3,4,5] to determine the electron density distribution over blunt sphere cone bodies at hypersonic speed to non-zero angle-of-attack of the body to the free stream. The behavior of the three dimensional laminar nonequilibrium boundary layer on blunt conical bodies is considered with emphasis on chemical nonequilibrium aspect of the air species and in particular, the production of electron. As in the previous studies diffusion of the dissociated and ionized air species with finite rate chemistry is also emphasized. Numerical results are given for the AFCRL Trailblazer body.

- 4 -

In Section II the equations of motion are given for the flow of a three
dimensional boundary layer in an orthogonal curvilinear coordinate system
appropriate for a sphere-cone body at angle-of-attack. These equations are
valid for a multi-component mixture of dissociated and ionized gas species
which may be reacting with each other with finite chemical rates. Viscosity,
heat conduction, and diffusion are the principal transport phenomena included
in the formulation. The boundary layer developing over the body is acted upon
by the outer inviscid flow which provides the edge conditions under which the
boundary layer develops. One complication as considered in reference (3) is
the swallowing of the streamlines with different entropy downstream of the
stagnation region.

Section III contains the inviscid flow analysis; considerations are given
to formulating the appropriate set for the three dimensional boundary layer edge
conditions. A numerical method of solution is provided for the three dimensional
flow of a chemical reacting gas. Numerical results for the edge conditions are
discussed in Section V and are given for a air mixture with finite reacting chem-
istry. Section IV summarizes the chemical rate constants, thermodynamic, and
transport properties for a dissociating and slightly ionized air mixture at high
temperature which are used in this study.

This report contains the equations utilized in the study and numerical re-
sults for boundary layer viscous flow at the stagnation line for bodies at non-
zero angle-of-attack. Numerical results are given for the edge conditions due
to the three dimensional inviscid flow. Further numerical results will be given
in a subsequent report.

II. Equations of Motion for Three Dimensional Laminar Boundary Layer

The problem of concern is the flow of a three dimensional boundary layer over a body at angle-of-attack at hypersonic speeds with transport processes and chemical reaction between dissociated and ionized air species. Since species of different molecular weight are present diffusion and convection of each species dominates the electron density at any point of the body. To date all studies of three dimensional boundary layer theory have emphasized non-reacting perfect gases. These have been reviewed, for example, in the article by Mager[9] and a more recent one by Eichelbrenner[10].

It is convenient to use a set of orthogonal curvilinear coordinates where the surface of the body is normal to one of the coordinates. With this normal coordinate the concept of a thin viscous layer developing over the surface can be utilized for obtaining the boundary layer equations from the Navier-Stokes equations of flow. With this set of coordinates the line element assumes the form.

$$ds^2 = h_1^2 dx^2 + h_2^2 dy^2 + h_3 dz^2 \qquad (2.1)$$

where x and z are the surface coordinates and y is normal to the body surface and the metric coefficients h_1, h_2, and h_3 are functions only of x and z when the boundary layer is thin compared to the principal radii of curvature of the surface. By setting $h_2 = 1$, y becomes the normal distance to the surface and it remains to choose the orthogonal surface coordinates. It is convenient for this study to

utilize the system of geodesic coordinates (Moore [11]) which simplifies the scale factor further to $h_1 = 1$ and the second one an arbitrary scale function $h_3 = r (x, y)$. For rotationally symmetric bodies such as sphere cones x is measured along the body generator, z the meridional angle, and $h_3 = r (x)$ is the radius of the body. Thus the only non-unit metric coefficient is r (x). This system of coordinate is the same as that used in the zero angle-of-attack study [3]. For any other more general body the set of orthogonal curvilinear coordinates can be obtained by a selection of one family and then obtaining the orthogonal projections by numerical computation.

In this set of coordinates where x is along the meridian curve, z is the meridional angle, and y is the distance normal to the surface. The equations for the conservation of momentum, energy, and species for the boundary layer are respectively given by:

$$\rho \left(\frac{du}{dt} - \frac{w^2 r'}{r} \right) = -\frac{\partial p}{\partial x} + \frac{\partial}{\partial y} \left(\mu \frac{\partial u}{\partial y} \right) \qquad (2.2)$$

$$\rho \left(\frac{dw}{dt} + \frac{u w r'}{r} \right) = -\frac{1}{r} \frac{\partial p}{\partial z} + \frac{\partial}{\partial y} \left(\mu \frac{\partial w}{\partial y} \right) \qquad (2.3)$$

$$\rho \bar{c}_p \frac{dT}{dt} = u \frac{\partial p}{\partial x} + \frac{w}{r} \frac{\partial p}{\partial z} + \mu \left[\left(\frac{\partial u}{\partial y} \right)^2 + \left(\frac{\partial w}{\partial y} \right)^2 \right] + \frac{\partial}{\partial y} \left(k \frac{\partial T}{\partial y} \right) + \sum_{i=1}^{N} \rho D_i \frac{\partial c_i}{\partial y} \frac{\partial h_i}{\partial y} \qquad (2.4)$$

$$- \sum_{i=1}^{N} w_i h_i$$

$$\rho \frac{dc_i}{dt} = \frac{\partial}{\partial y} \left(\rho D_i \frac{\partial c_i}{\partial y} \right) + w_i \quad , \quad i = 1, 2, \ldots N \qquad (2.5)$$

In the above equations the operator is defined by

$$\frac{d}{dt} = u \frac{\partial}{\partial x} + \frac{w}{\pi} \frac{\partial}{\partial z} + v \frac{\partial}{\partial y}$$

The prime denotes differentiation with respect to x and N is the maximum number of species. In these equations the symbols have the following meaning: u, v, and w are the velocity components along the x, y, z coordinates respectively; ρ, k, μ, $\bar{c}_p$ are the mass density, heat conductivity, viscosity coefficient, and specific heat coefficient at constant pressure of the gas mixture; D_i (i = 1, 2. ...N) are the binary diffusion coefficients. These gas properties are functions of the temperature T and of the species concentration c_i in mass fraction units. The production and loss of species through dissociation and recombination is indicated by the term w_i which is the mass rate of production of the ith species per unit volume for each reaction. In general, the left side of these equations are the change of the quantities concerned due to convective processes and are balanced by the diffusive effects such as viscosity, diffusion and heat conduction. Conservation of momentum normal to the surface is satisfied by the condition for the constancy of the pressure in this direction. In addition to these equations the pressure is given by the equation of

state for the gas mixture and is given by:

$$p = R \rho T \sum_{i=1}^{N} \frac{c_i}{M_i}$$

(2.6)

where R is the universal gas constant, M_i is the species molecular
weight. The species of interest in this study those from dissociated
and ionized air which may numbered to 10 for the neutrals and their
positive ion.

The species equation satisfy a global conservation of mass given
by

$$\frac{\partial}{\partial x}(\rho u \hbar) + \frac{\partial (\rho w \hbar)}{\hbar \partial \hbar} + \frac{\partial}{\partial y}(\rho v \hbar) = 0$$

(2.7)

These equations together with chemical rate constants, thermodynamics,
and transport properties described in Section IV are sufficient to de-
termine the $(4 + N)$ unknowns. Due to the constancy of the pressure
through the boundary layer the pressure is prescribed by the inviscid
flow outside of the boundary layer.

From the problem as stated above the flow at angle-of-attack over
a rotationally symmetric body such as a sphere-cone combination has
symmetry with respect to the plane containing the free stream velocity
vector and a body meridian curve. The meridian curve containing the
stagnation point of the flow is a line of symmetry and the velocity
component w normal to this curve along the body is zero. One notes
also that the equations for a set of wind oriented coordinate con-
structed at the stagnation point when it is on the sphere reduces

immediately to the same form as that of the zero angle-of-attack case. With consideration of a boundary layer concept the gradients normal to the surface dominate the diffusive processes due to viscosity, heat conduction, and species diffusion. The implication of this is that the differential system remains parabolic and the characteristics at any point of the flow are changed only by upstream conditions. However, a complication of the three dimensionality appears in that the streamlines do not remain in the same meridian plane and imposes a condition on the computational aspect of the problem.

For a sphere cone body at non-zero angle-of-attack to the free stream the flow over most of the spherical part of the body is symmetric about an axis parallel to the free stream. That is, the stagnation point of the flow remains on the sphere if the angle-of-attack is less than the complement of the cone angle. This condition is satisfied for the values of angle-of-attack for which the three dimensional laminar boundary layer equations are valid. The origin of the coordinates x, y and z is located at the nose of the sphere cone body. This is the body oriented set of coordinates. At the stagnation point another set of coordinates can be constructed which is wind oriented. The spherically symmetric solutions obtained for the zero angle-of-attack case are valid in this set of coordinates. By this mean the flow characteristics for the spherical portion of the flow can be obtained by the zero angle-of-attack assumption and utilized as initial conditions for the angle-of-attack case.

A further transformation is made to scale the growth of the boundary layer due to compressibility effect. This is given by

$$\eta = \left(\frac{u_e}{\rho_r \mu_r \alpha(\xi, \zeta)} \right)^{1/2} \int_o^y \rho \, dy$$

$$\xi = \xi(x - \alpha_D R_N) \quad , \quad \zeta = z \qquad (2.8)$$

In this set of coordinates ξ, η are the transformed coordinates along and normal to the meridian and ζ is the meridional angle. The application of this transformation (7) to equation (1) to (5) lead to the following:

$$\alpha f' \frac{\partial f'}{\partial \xi} \xi_x + \frac{w}{u_e} \frac{\alpha}{r} \frac{\partial f'}{\partial \zeta} + V \frac{\partial f'}{\partial \eta} + \frac{\alpha}{u_e} \left(f'^2 u_e \frac{\partial u_e}{\partial \xi} \xi_x \right.$$
$$\left. + \frac{1}{\rho} \frac{\partial p}{\partial x} \right) + \frac{w}{r} \frac{\alpha}{u_e^2} f' \frac{\partial u_e}{\partial \zeta} - \alpha \frac{w^2}{u_e^2} \frac{r'}{r} = \frac{\partial}{\partial \eta} \left(\ell \frac{\partial f'}{\partial \eta} \right)$$

$$(2.9)$$

$$\alpha f' \frac{\partial \vartheta}{\partial \xi} \xi_x + \frac{w}{u_e} \frac{\alpha}{r} \frac{\partial \vartheta}{\partial \zeta} + \frac{\alpha \vartheta}{T_e} \left(f' \frac{\partial T_e}{\partial \xi} \xi_x + \frac{w}{u_e r} \frac{\partial T_e}{\partial \zeta} \right)$$
$$+ V \frac{\partial \vartheta}{\partial \eta} = \frac{\alpha}{\rho \bar{c}_p T_e} \left(f' \frac{\partial p}{\partial \xi} \xi_x + \frac{w}{u_e r} \frac{\partial p}{\partial \zeta} \right) +$$
$$\frac{\ell u_e^2}{\bar{c}_p T_e} \left[\left(\frac{\partial f'}{\partial \eta} \right)^2 + \left(\frac{\partial (w/u_e)}{\partial \eta} \right)^2 \right] +$$
$$\frac{1}{\bar{c}_p} \frac{\partial}{\partial \eta} \left(\frac{\ell \bar{c}_p}{P_r} \frac{\partial \vartheta}{\partial \eta} \right) + \frac{\ell}{\bar{c}_p P_r} \frac{\partial \vartheta}{\partial \eta} \sum_{i=1}^N Le_i c_{p_i} \frac{\partial c_i}{\partial \eta}$$
$$- \frac{1}{\bar{c}_p} \sum_{i=1}^N \frac{\alpha}{u_e T_e} \frac{w_i}{\rho} h_i \qquad (2.10)$$

$$\alpha\, u_e\, f' \frac{\partial w}{\partial \xi} \xi_x + \alpha \frac{w}{\hbar} \frac{\partial w}{\partial \zeta} + V u_e \frac{\partial w}{\partial \eta}$$

$$+ \alpha f' w u_e \frac{\hbar'}{\hbar} = -\frac{\alpha}{\rho} \frac{\partial p}{\hbar \partial \zeta} + u_e \frac{\partial}{\partial \eta} (\ell \frac{\partial w}{\partial \eta}) \qquad (2.11)$$

and the species equation for each species

$$\alpha f' \frac{\partial c_i}{\partial \xi} \xi_x + \frac{w \alpha}{u_e \hbar} \frac{\partial c_i}{\partial \zeta} + V \frac{\partial c_i}{\partial \eta} = \frac{\partial}{\partial \eta} (\ell \frac{\mathcal{L}_{e_i}}{P_\hbar} \frac{\partial c_i}{\partial \eta})$$

$$+ \frac{\alpha}{u_e} \frac{w_i}{\rho} \qquad (2.12)$$

The function V is given by the global equation of mass (6)

$$\frac{\partial V}{\partial \eta} = -\alpha \frac{\partial f'}{\partial \xi} \xi_x - f' \xi_x \alpha \left[\frac{1}{u_e \hbar} \frac{\partial (u_e \hbar)}{\partial \xi} - \frac{1}{2 u_e} \frac{\partial u_e}{\partial \xi} \right.$$

$$\left. - \frac{1}{\rho_r \mu_r \alpha} \frac{\partial (\rho_\hbar / \mu_\hbar \alpha)}{\partial \xi} \right] - \frac{\alpha w}{\hbar^2 \zeta u_e^2} \frac{\partial (\zeta \hbar w_e)}{\partial \zeta}$$

$$\qquad (2.13)$$

$$- \frac{\zeta \alpha}{\hbar} \frac{\partial}{\partial \zeta} \left(\frac{w}{\zeta u_e}\right) + \frac{\zeta}{2\hbar} \left(\frac{w}{\zeta u_e}\right) \left[\frac{\alpha}{u_e} \frac{\partial u_e}{\partial \zeta} \right.$$

$$\left. - \frac{1}{\rho_\hbar \mu_r} \frac{\partial}{\partial \zeta} (\rho_r / \mu_r) \right]$$

- 12 -

Equation (13) is obtained from the conservation of mass (6) by noting that the latter is satisfied by a vector potential whose derivatives lead directly to the physical velocity components. A transformation of the coordinate then leads to equation (13). In these equations the notation is as follows:

$$f' = u/u_e \; , \quad \ell = (\rho \mu)/(\rho_r \mu_r) \, , \quad \mathcal{L}_{e_i} =$$

$$\rho \, D_i \, \bar{c}_p / k \quad \text{is the Lewis number,} \quad P_r = \mu \, \bar{c}_p / k$$

is the Prandtl number, $\vartheta = T/T_e$. The subscript e denotes values at the boundary layer edge and are obtained from the inviscid flow as given in Section III. In addition, the V function is a combination of the velocity components of the form:

$$V = \alpha \left(f' \eta_x + \frac{w}{r u_e} \eta_\zeta + \frac{v}{u_e} \eta_y \right) \tag{2.14}$$

In these equations α and ζ remain arbitrary function of their respective arguments and are assigned.

2.2 Method of Solution by Finite Differences

The method utilized for the solution of the three dimensional boundary layer equations as set forth in the previous section is the finite difference one. The coupled, nonlinear, partial differential equations are quasi-linear with second order derivatives in one direction only, namely, the direction y normal to the surface of the body. Thus these equations remain parabolic with non-zero angle-of-attack as in the two dimensional case. The three dimensionality of the flow at angle-of-attack leads to a cross-flow velocity component which tends to

- 13 -

sweep the flow around the body. Due to this factor the domain of dependence

of a given point depends on the spanwise mathematical characteristics of the

equations in a complicated way. One set of characteristics of this set of

equations is the streamlines or traces of the streamlines in planes parallel

to the surface of the body. These lines have a cross-flow direction to the

main free stream and carries disturbances from one part of the flow to another.

Disturbances are also propagated downstream by first diffusing normal from

the wall to the boundary layer edge where they are then carried downstream by

the external flow. The characteristics of the convective operator including

the cross-flow component lead to the Courant-Friedrich-Lewy condition of

$$\frac{\Delta z}{\Delta x} \geqslant \frac{w}{u} \quad . \tag{2.15}$$

This condition implies that domain of the difference scheme contains that of
the differential system [12] . The implication of this stability condition is

that difference schemes which are inherently stable such as implicit type are

now conditionally stable for three dimensional flow; the condition given by

equation (15) must be satisfied at each point.

The difference scheme of Crank-Nicolson or the fully implicit one has

been used in the zero angle-of-attack case. There have been a number of

generalization of these schemes (implicit and explicit) to consider the non-
zero angle-of-attack flows [13,14,15,16] . The principal problem which pre-

sents itself in three dimensional flow is the conditional stability introduced
by the angular momentum equation. Krause[13] has introduced a scheme where-

by reverse cross-flow can be considered. This can be useful for such cases.
A difference scheme related to the Crank-Nicolson[14] one for two dimensional

flow has been utilized in this study. A similar scheme was utilized by Lew

for the study of chemically reacting gases and solids with time dependency.

The scheme averages the derivatives in the normal direction and angular direc-

tion in such a way that the algebraic equations are tri-diagonal. Consider a

three dimensional rectangular grid with grid lines parallelling the x, z, y

axes with the indices 1, m, n along the x, z, and y directions respectively.

The represnetative second order equation for either the velocity, temperature,

or species concentration can be given by

$$\Phi_{\eta\eta} = F(\xi, \zeta, \eta; \Phi, \Phi_\xi, \Phi_\eta, \Phi_\zeta) \qquad (2.16)$$

where Φ is any of the dependent variables. The finite difference re-

presentations are then

$$\Phi_{\eta\eta} = \frac{1}{2}\left(\frac{\partial^2}{\partial\eta^2}\Phi(\ell+1, m+1, n) + \frac{\partial^2}{\partial\eta^2}\Phi(\ell, m, n)\right)$$

$$\Phi_\xi = \frac{1}{2}\left(\frac{\partial\Phi}{\partial\xi}(\ell+\tfrac{1}{2}, m+1, n) + \frac{\partial\Phi}{\partial\xi}(\ell+\tfrac{1}{2}, m, n)\right)$$

$$\Phi_\eta = \frac{1}{2}\left(\frac{\partial\Phi}{\partial\eta}(\ell+1, m+1, n) + \frac{\partial\Phi}{\partial\eta}(\ell, m, n)\right)$$

$$\Phi_\zeta = \frac{1}{2}\left(\frac{\partial\Phi}{\partial\zeta}(\ell+1, m+\tfrac{1}{2}, n) + \frac{\partial\Phi}{\partial\zeta}(\ell, m+\tfrac{1}{2}, n)\right)$$

These equations for the difference representation lead to difference
equations involving the three values of n along two surface normals diagonal
to each other and two known additional points. The finite difference
scheme leads to a tri-diagonal scheme for three unknowns for each equation
at the points along the normal passing through $\ell + 1$ and $m + 1$. The
central differences are used for the first derivatives. Any instability
in the implicit scheme arises from the cross-flow in the m index direction.
The first derivatives with respect to the normal distance are evaluated
at diagonal points instead of at the four vertices of the rectangle as pres-
cribed by the Crank-Nicolson scheme. Krause (13) utilizes a forward point
difference of the cross derivative and can account for reverse cross-flow.
This would be a simple addition to the present scheme. The tri-diagonal
algebraic equation can be written in the form:

$$A_n W_{n+1} + B_n W_n + C_n W_{n-1} = D_n \qquad (2.17)$$

and can be solved by a simple algorithm (12). The coefficients A_n, B_n, and
D_n are obtained from one sweep progressing in n; then the unknown w_n is
obtained from a second sweep starting from the maximum value of n. Thus,

$$W_n = E_n W_{n+1} + e_n \qquad (2.18)$$

where

$$E_2 = - (A_2 + C_2 F)/(B_2 + C_2 H)$$

$$e_2 = (D_2 - C_2 H)/(B_2 + C_2 H)$$

$$E_n = -A_n/(B_n + C_n E_{n-1})$$

$$e_n = (D_n - C_n e_{n-1})/(B_n + C_n E_{n-1})$$

for $3 \leq n \leq N-1$ where N is the maximum number of points used.
The boundary conditions are given in the same form and can be written as

$$W_1 = HW_2 + FW_3 + h$$

$$W_N = g$$

in terms of the boundary values coefficients of H, F, h, and g. The
solution involved in the above is valid for a set of linear algebraic
equations. The set of nonlinear differential equations from which the
finite difference equations were obtained was linearized first by the
concept of quasi-linearization. This quasi-linearization is required
for the chemical production terms in both the species and energy equa-
tions and in the nonlinear convective terms.

2.3 **Initial Conditions**

For the sphere cone body with a large nose radius such as the
Trailblazer body the stagnation point will locate itself on the spheri-
cal portion of the body for a large range of values of the angle-of-
attack. The flow over the sphere is symmetric with respect to the wind
coordinates when the stagnation point is located there. The relative
coordinate systems are shown on Figure 2.1. The set of equations as given
in Section 2.1 can also be utilized for the flow with respect to the wind
coordinates; it reduces, of course, to the two dimensional flow (at zero
angle-of-attack) considered previously in reference (3). The wind coordinate
symmetric flow solution will be utilized as initial conditions for the flow
at non-zero angle-of-attack at a point where both solutions are valid. This
usually occurs at the shoulder juncture on the windward meridian. The inter-
section of the streamlines from the stagnation point with each meridian pro-
vides the angular displacement of the velocity components u and w. Since there

is no variation of characteristics across streamlines in the symmetric portion of the flow the conditions at the initial line are obtained by an interpolation for each point of one set of zero angle-of-attack solutions. The velocity in the angular direction for the body oriented coordinates involve a component of axial velocity dependent on the angle-of-attack and body location.

III. <u>Inviscid Flow for Edge Boundary Conditions</u>

As indicated in Section II the edge values of the flow velocities, temperature, and species concentration are required. These values are usually obtained from considerations of the inviscid equations for three dimensional flow. Since only the edge values are needed approximations by means of utilizing experimental fits of pressure distribution or its Newtonian approximation have been found adequate for the zero angle-of-attack case. For a slightly blunted conical body streamlines entering the downstream boundary layer edge are not the body streamline and an experimental fit of the shock shape has been found sufficient to obtain the effect of entropy gradient in the inviscid flow. This method of obtaining the edge conditions has been utilized for the symmetric portion of the flow (reference 3).

3.1 <u>Edge Conditions at Surface of Body at Angle-of-Attack</u>

The edge conditions for the non-symmetric portion of the body require a more complicated analysis because of the additional degree-of-freedom. For the first step the body streamline characteristics are obtained by utilizing the solution of the three dimensional equations of motion and prescribed pressure distributions over the entire body. The solution involves the set of momentum, energy, and species equations for a chemical reacting finite rate chemistry multicomponent gas with dependency on the two surfaces coordinates x and z. An iterative finite difference scheme has been chosen for the method of solution.

The equations of motion at the surface of the body for an inviscid flow can be obtained from equations (2.2) to (2.5) by setting the transport

terms to zero. At the surface, y = o and the normal component v of the velocity is also zero. Thus the operator d/dt becom simply

$$\frac{d}{dt} = u_e \frac{\partial}{\partial x} + \frac{w_e}{\hbar} \frac{\partial}{\partial z}$$

where the subscript e denotes the inviscid edge values for the boundary layer. These equations are then

$$\frac{d u_e}{dt} - \frac{w_e^2 \hbar'}{\hbar} = -\frac{1}{\rho_e} \frac{\partial}{\partial x} p_e \tag{3.1}$$

$$\frac{d w_e}{dt} + u_e w_e \frac{\hbar'}{\hbar} = -\frac{1}{\rho_e \hbar} \frac{\partial p_e}{\partial z} \tag{3.2}$$

$$\frac{d T_e}{dt} = \frac{1}{\rho_e \bar{c}_p} \left(u_e \frac{\partial p_e}{\partial x} + \frac{w_e}{\hbar} \frac{\partial p_e}{\partial \zeta} - \sum_{i=1}^{N} w_i h_i \right) \tag{3.3}$$

$$\frac{d c_{ie}}{dt} = \frac{w_{ie}}{\rho_e} \quad , \quad i = 1, 2, \dots N . \tag{3.4}$$

In addition, the equation of state as given by equation (2.6) is used to relate the pressure to the other thermodynamic variables. The enthalpy and chemical production terms are the same as described in Section 2.

For conditions at the body surface the pressure distribution is prescribed by a modified Newtonian law dependent on the flow deflection at the particular point. Reliable pressure value on the body surface are

usually obtained from a modified Newtonian theory at high deflection angles. Der[15] has suggested an improvement of the surface pressure at the smaller deflection angle ($< 45°$) on the basis of experimental data and characteristics solutions for a sphere-cone (NASA) and this is approximated by the equation of

$$\frac{C_p}{C_{p_{MAX}}} = \frac{1}{1 + exp\left[4\left(\theta - \frac{\pi}{4}\right)\right]} \quad , \quad \theta \geqslant \frac{\pi}{4} \qquad (3.5)$$

$$\frac{C_p}{C_{p_{MAX}}} = \cos^2\theta \quad , \quad \theta < \frac{\pi}{4} \qquad (3.6)$$

where θ is the complement of the flow deflection angle and C_p is the coefficient of pressure. Equations (3.5) and (3.6) are matched at $\theta = \pi/4$.

With the pressure distribution at each point of the body surface given by equations (3.5) and (3.6) the inviscid edge flow can be obtained from equations (3.1) to (3.4). There are $(3 + N)$ unknowns of u_e, w_e the two velocity components, T_e the temperature and C_{i_e} $(i=1,2,...N)$ the species concentration in mass fraction. These nonlinear partial differential equations are first order and require a different method of solution from the previous section. This is discussed in the next section. The values of the dependent variables are prescribed at the initial line. This is sufficient to provide the solution at any other point. For the study here the initial line is chosen normal to its body symmetry axis, that is, in the body oriented coordinate. As

described in the previous section this initial line intersects the streamlines issuing from the stagnation point at different points along their flow (See Fig. 2.1). The velocity components at this initial line are given in terms of the wind oriented coordinate solutions.

The relation between a wind-oriented coordinates which has its origin at the stagnation point and a body-oriented with its origin at front symmetry point can be given by a set of equations:

$$\cos\left(\frac{s}{R_N}\right) = \sin\alpha_D \cos\zeta \sin\left(\frac{x}{R_N}\right) + \cos\alpha_D \cos\left(\frac{x}{R_N}\right)$$

$$\cos\gamma \sin\left(\frac{s}{R_N}\right) = \cos\alpha_D \cos\zeta \sin\left(\frac{x}{R_N}\right) - \sin\alpha_D \cos\left(\frac{x}{R_N}\right)$$

$$(3.7)$$

These equations are valid for a body at an angle-of-attack α_D to the free stream and x, s denote the distance along the body measured from the body origin and stagnation point respectively and where ζ , γ denote the angular displacement with respect to the corresponding axes. It is noted that these quantities become equal when $\alpha_D = 0$, the zero angle-of-attack case. Equations (3.7) transform the initial profiles which are symmetric with respect to the wind-oriented axes into the body-oriented coordinates. The flow characteristics are symmetric for constant value of s for the wind-oriented coordinates and provide the initial conditions at each body meridian.

3.2 Method of Solution of Inviscid Edge Vallues

The prescription of the pressure distribution by equations (3.5) and

(3.6) with the deflection angle obtained from equations (3.7) leads

directly to the pressure gradients required for the solution of

equations (3.1) to (3.4). These equations constitute a nonlinear

first order set of partial differential equations in two directions.

They are solved by a predictor-corrector method such as used by Mac-

Cormack [19]. In this scheme the solution can be predicted by

$$\widetilde{F}(m, \ell+1) = F(m, \ell) - A(m, \ell) \left[F(m+1, \ell) \right.$$
$$\left. - F(m, \ell) \right] \Delta \xi / \Delta S + G(m, \ell) \Delta \xi \tag{3.8}$$

and corrected by

$$F(m, \ell+1) = \frac{1}{2} \left\{ F(m, \ell) + \widetilde{F}(m, \ell+1) \right.$$
$$- A(m, \ell+1) \left[\widetilde{F}(m, \ell+1) - \widetilde{F}(m-1, \ell+1) \right].$$
$$\left. \cdot \Delta \xi / \Delta S + \widetilde{G}(m, \ell+1) \Delta \xi \right\} \tag{3.9}$$

This method is useful for flows where convection dominates the situation

and is stable provided the CFL condition is satisfied. In this case the

criterion for stability is given by

$$\Delta \xi \le \Delta S / A(m, \ell) \tag{3.10}$$

and is satisfied by all the equations at each point of the grid. In

equations (3.8) and (3.9) ℓ and m are the indices along the meridian curve

measured by ξ from the stagnation point ($\xi = x - \alpha_b R_N$ for inviscid

flow considered in this section) and along the angular displacement measured

by S. The coefficients A and G are given by each individual equations

(3.1) to (3.4).

Initial conditions are required $m = 1$ along the stagnation line and at a value of $\ell \neq 1$. At the stagnation line and the leeward symmetry line the flow has zero angular velocity due to symmetry. Thus the velocity component we is zero and equation (3.1) to (3.4) reduces to flow along the streamline. These equations along the streamlines are again integrated by a predictor-corrector of the same form as equations (3.8) and (3.9) except that there is only one coordinate involved.

The initial conditions for all the three dimensional equations are obtained from the inviscid flow for the front portion of the sphere

IV. Chemical, Thermodynamics and Transport Gas Model

4.1 Chemical Kinetic Rate Constants

The chemical kinetics system for a nitrogen-oxygen atmosphere is of concern for Trailblazer II conditions. The flight regime involves principally velocities $\sim$ 17,500 ft/sec. Since there is no ablation of body material the gas mixture is composed of dissociated and ionized air speies. For most cases these species are O_2, N_2, N. O. NO, NO^+ and electrons. The higher temperature range to $15,000^{\circ}K$ for altitudes around 100 km requires the additional atomic and molecular ions of N_2^+, O_2^+, N^+, and O^+. The chemical system involving the neutral species and NO^+ is given in reactions 1 to 6 in Table I which also contains additional reactions which become important at the higher temperature range of $15,000^{\circ}K$. This Table of reactions has been suggested by Bortner[20] for a nitrogen-oxygen system typical of the shock layer of re-entry bodies. At a higher temperatures the assoicative ionization reaction 7 and 8 and collisional ionization reactions for the neutral species as given by 9 to 13 become important. Finally, after the formation of the positive ions, exchange reactions redistribute these charges by means of reactions 14 to 20. The reaction rate constants have been suggested by Bortner in Reference (21) and (22) where he also discusses their uncertainties and limitations. Results in this report are obtained using reactions 1-6 and reactions 1-10, 14, 15, 17, 18, 20. A minimum number of reactions consistent with reality is utilized.

In general, the chemical reactions are represented by the equation

$$\sum_{i=1}^{N} \alpha_{ri} X_i \rightleftharpoons \sum_{i=1}^{N} \beta_{ri} X_i \qquad (4.1)$$
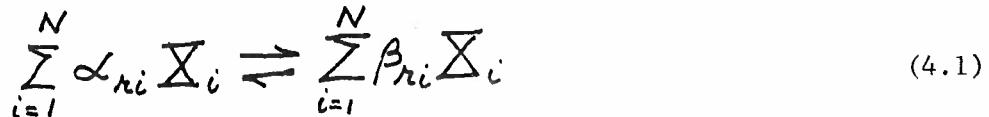
where the subscript r represents the particular reaction, i is the species that is being reacted and α_{ri}, β_{ri} are the stoichiometric coefficients. In this report the values of r and i range over the number of reactions and the number of species respectively. For this representation the net mass rate of production of species i per unit volume can be immediately given by

$$W_i = M_i \sum_{k=1}^{R} (\beta_{ri} - \alpha_{ri}) \left[k_{fr} \prod_{j=1}^{J} \left(\frac{\rho c_j}{M_j} \right)^{\alpha_{rj}} - k_{br} \prod_{j=1}^{J} \left(\frac{\rho c_j}{M_j} \right)^{\beta_{rj}} \right] \quad (4.2)$$

In this equation M_i is the molecular weight of species 1 and the subscript j denotes the species and the catalytic bodies, i.e, j = 1, 2, ...N, N+1, ... J. The mass fraction of catalytic bodies is given in terms of the N species by

$$c_j = M_j \sum_{i=1}^{J} z_{(j-N), i} \, c_i / M_i \quad (4.3)$$

for j = N + 1, ... J. The use of equation (4.3) facilitates the computation problem for large systems of chemical species and flow variables.

Equation (4.2) is the source term for the mass generation of species and is a function of the density ρ of the mixture, the temperature T, and the density (ρc_i) of the pertinent species. The rate constants k_{fr} and k_{br} are, of course, functions of the temperature T.

4.2 Thermodynamic

The gas model is composed of air species and reactions as considered above. The total enthalpy of the air mixture is easily obtained when

the individual species values are first made available. For the chemical

reacting gas mixture, the enthalpy is obtained by the summation

$$h = \sum_{i=1}^{N} c_i h_i \qquad (4.4)$$

where the pure species enthalpy values have been tabulated by Browne[23].

The thermodynamic properties for the diatomic molecules were obtained

from the second virial coefficient approach which essentially leads to

the thermodynamic properties departure from the monatomic gas at the

higher temperature; the Morse potential is utilized. At the lower temper-

ature, the diatomic species are considered as rigid rotator harmonic os-

cillators with corrections for rotational stretching and vibrational an-

harmonicity. Comparison of these data with others are excellent and have

been given by Browne[23]. The individual species values of the enthalpy

are given in Figure (4.1).

The mixture specific heat is obtained similarly as

$$\overline{C}_p = \sum_{i=1}^{N} c_i C_{p_i} \qquad (4.5)$$

4.3 Transport Properties

The transport properties involve the coefficients of viscosity and

conductivity. The individual species coefficients have been obtained

from a number of sources. The species viscosity in terms of the collision

integrals $\Omega_i^{(2,2)}$ is given by the relation:

$$\mu_i = 26.693 \times 10^{-6} \frac{(M_i T)^{1/2}}{\Omega_i^{(2,2)}}, \text{ poises} \qquad (4.6)$$

- 27 -

Collision integrals from Yun and Mason [24] for dissociated air species are utilized in the compututations; the integrals are dependent on the intermolecular potential.

The conductivity k_i of the species is related to μ_i by

$$k_i = \frac{\mu_i R}{M_i} \left[C_{p_i} \frac{M_i}{R} + 1.25 \right]$$

where k_i is in g-cal per (cm sec$^\circ$ K).

Finally, the mixture values of the viscosity and conductivity are given by Wilke's rules whereby

$$\mu = \sum_{i=1}^{N} \left(\frac{X_i \mu_i}{\sum_{j=1}^{N} X_j \phi_{ij}} \right) \tag{4,7}$$

$$k = \sum_{i=1}^{N} \left(\frac{X_i k_i}{\sum_{j=1}^{N} X_j \phi_{ij}} \right)$$

where $X_i = c_i M/M_i$

$$\phi_{ij} = \frac{\left[1 + \sqrt{\frac{\mu_i}{\mu_j}} \left(\frac{M_i}{M_j} \right)^{1/4} \right]^2}{\sqrt{8} \sqrt{1 + \frac{M_i}{M_j}}} \tag{4.8}$$

V. Numerical Results

Some numerical results are given in this section; detailed flow field calculations will be presented in a separate data memorandum. These results were obtained with the following considerations. The six species O_2, N_2, NO, N, O, and NO^+ with reactions 1 to 6 were used. For the angles-of-attack of interest the stagnation point of the flow lies on the spherical portion of the body resulting in a region of symmetrical flow. The distributions of flow characteristics for flows with symmetry (at zero angle-of-attack) have been given in the previous report (Lew[3]). These results are used as initial conditions for the three dimensional flow considered herein. One notes that the three dimensional boundary layer program can also be initiated directly at the stagnation point by generating its own intial profiles by appropriate use of the proper coordinates. By utilizing the two dimensional symmetrical flows as initial conditions there is a slight saving in cost. Moreover, the effect of swallowing for the front portion of the flow is accounted for by this means.

The pressure distribution utilized in this report is a first approximation. Previous results in reference (2) and (3) use a next approximation to the inviscid edge conditions. These conditions are valid for a thin shock layer with pressure variation across the shock layer given by the first integral of the momentum equal normal to the surface. This integral is given by

$$p(x, \psi) = p_s(x) - \int_\psi^{\psi_s} \frac{u}{R_c r} d\psi \qquad (5.1)$$

- 29 -

where $p_s(x) = p(x, \psi_s)$ is the pressure at the shock, ψ is the stream function (this may be measured with respect to the body where it has a value of o) and u, R_c, r are the tangential velocity, radius of curvature, and the local radius around the axis of symmetry respectively. Consistent with the approximation of this thin shock layer theory, the integral is evaluated at the shock. This fact simplifies equation (5.1) to the form:

$$p(x, \psi) = p_s(x) - (p_B(x) - p_s(x))\left(\frac{\psi}{\psi_s(x)} - 1\right) \qquad (5.2)$$

where the subscripts B and S denote values evaluated on the body and shock respectively. This relation was used for the next approximation to the pressure in the previous two dimensional results,[2] see also Lew[25] for further discussion and derivation. The use of relation (5.2) require a shock shape at each flight condition and a number of experimental and analytical results of shock shape for hypersonic flow over sphere-cone at zero angle-of-attack was correlated and used. As the results of reference (3) show, the pressure for a blunted cone drops rapidly at the shoulder dependent on the cone angle, overexpands below the downstream conical values and then rises asymptotically to these latter values. Dissociated atomic species decay rapidly prior to the shoulder having increased for a short distance from the stagnation point. The species concentration after the initial point considered here are those for the body streamline after a partial swallowing has been accounted for.

As examples the inviscid edge values of velocity, temperature, and species concentration were obtained fro the case of the AFCRL Trailblazer body at 240,000 ft. altitude flying at 17,500 ft./sec. for non-zero values of angle-of-attack. These values are 2, 6 and 12 degrees. Since there is symmetry in the plane of the velocity vector only the variation from $S = 0$ to π is considered. Initial conditions were obtained from reference (2). Results are given on Figures (5.1), (5.2) and (5.3) for the cases of angles-of-attack indicated. In Figure (5.1) the variation of the angular velocity component around the body shows a peak at about 90 degrees azimuthal angle. This peak increases with angle-of-attack. This means that the streamlines have their largest directional deviation from the axis of symmetry at this point and gradually align themselves to the leeward line of symmetry and then proceed downstream. The angular displacement of the streamline from the meridian plane is given by $\tan^{-1}(w_e/u_e)$. There is a drop of temperature in the azimuthal direction as expected; the pressure is lower on the leeward side. The axial velocity changes little from the windward to leeward planes. Figure (5.2) shows the variation of w_e with angle-of-attack. These results behave qualitatively as the sharp cone at non-zero angle-of-attack to the flow. The atomic oxygen distribution around the body at $x = 2.4$ ft. is given in Figure (5.3) and shows only a small variation.

The edge values of the inviscid flow have been discussed above. These have been utilized as boundary conditions for the three dimensional boundary layer. The same number of species and reactions is used in this illustrative example. Gradients for the edge characteristics from the inviscid flow are obtained by a cubic spline fit for the stagnation line and a bicubic spline fit for the three dimensional aspect of the boundary layer. Typical results are shown in Figure (5.4) and (5.5). The gradient of the angular velocity is nonzero along the stagnation streamline and is defined by

$$ g' = \frac{w_e}{\varsigma u_e} \left(\frac{w}{w_e} - f' \right) $$

One notes that the angular velocity component w is zero at the stagnation streamline to the first power of the angular displacement ς. Thus the ratio w/w_e has a nonzero value there. The quantity $(w_e / \varsigma u_e)$ has values which vary at x = .48 ft. from 0.181 for 6° angle-of-attack to 0.409 for 12° angle-of-attack. This parameter gives an idea of the increasing angular velocity as compared to the axial velocity for increasing angle-of-attack. The variation of g' across the boundary layer is shown in Figure (5.4). The slight variation for small values of x increases downstream to an order-of-magnitude at x = 2.55 ft. Deviation of the axial streamlines from the windward rays to the leeward side is thus indicated. g' is, of course, zero in two dimensional symmetrical flow. The electron density distribution for two values of x are shown on Figure (5.5). The effect of angle-of-attack and the pressure distribution is evident from the figure. It is remembered that the boundary edge values for

the three dimensional case are evaluated at the body streamline after a partial swallowing has occurred.

VI. Concluding Remarks

The problem of determining the electron density distribution in the shock layer of re-entry bodies in hypersonic flight for nonzero angle-of-attack has been considered. This report constitutes Part I of a series of report on three dimensional effects. In this first part the complete governing system of equations for the flow of an ionized and dissociated air three dimensional boundary layer and the geometrical considerations have been given together with the transport and thermodynamics model, and kinetic rate constants utilized. In addition, equations are developed for a given pressure distribution for the determination of the edge values required for the solution of the boundary layer equations. Finite difference methods have been utilized for both the solution of the boundary layer and the inviscid flow necessary for the edge conditions. These methods are the implicit difference scheme and the predictor-corrector scheme respectively. In addition to the presentation of the model and system of equations this report also contains results for the three dimensional inviscid flow for several angles-of-attack and the results for the stagnation line boundary layer at nonzero angle-of-attack. Detailed evaluation of further results will be given in subsequent reports.

VII. <u>References</u>

1. Hayes, D. T. and Rotman, W., Microwave and Electrostatic Probe Measurements on a Blunt Re-entry Vehicle, AIAA Journal, Vol. 11, No. 5, 675-682 (1973).

2. Hayes, D. T., Herskovitz, S. B., Lennon, J. F., and Poirier, J. L., Prelimary Report on the Trailblazer II Chemical Alleviation Flight of 28 July 1972, AFCRL 72-0640, Oct 25, 1972.

3. Lew, H. G., Shock Layer Ionization at High Altitude, AFCRL 70-0702 (GE 70SD872), Nov. 1970.

4. Lew, H. G. Hypersonic Viscous Shock Layer Ionization at High Altitude, Data Memos A, 1, 2, 3 (GE) 1971-1972.

5. Lew H. G., A Study of Electron Density Distribution in Viscous Flows, AFCRL 72-0718, GE TIS 72SD 189, Nov. 1972.

6. Tracy, R. R., "Hypersonic Flow Over a Yawed Circular Cone", Memo No. 69 C.I.T., August 1963.

7. Stetson, K. F., "Experimental Results of Laminar Boundary Layer Separation on a Slender Cone at Angle of Attack at M = 14.2", ARL 71-0127, August 1971.

8. Rakich, J. V. and Cleary, J. W., "Theoretical and Experimental Study of Supersonic Steady Flow Around Inclined Bodies of Revolution", AIAA Journal, Volume 8, No. 3, 511-518 (1970).

9. Mager, A., Three-Dimensional Laminar Boundary Layer, Section C, Volume IV, High Speed Aerodynamics and Jet Propulsion, ed. F. Moore, Princeton Univ. Press, 1964.

10. Eichelbrenner, E. A., Three Dimensional Boundary Layers, Annual Review of Fluid Mechanics, Vol. 5, 1973.

11. Moore, F. K., Three-Dimensional Boundary Layer Theory, Advances in Applied Mechanics, Academic Press (1956).

12. Isaacson, E.,Keller, H. B., Analysis of Numerical Methods, John Wiley & Sons, Inc., 1966.

13. Krause, E., Herschel, E. H., and Bothmann, Th., Numerische Stabilität dreidimensionaler Grenzschichtlösungen, ZAMM, Vol. 48, No. 8, T205-T208, 1968.

14. Dwyer, H. A., Solution of a Three-Dimensional Boundary Layer Flow with Separation, AIAA J., Vol. 6, NO. 7, p 1336-1342 (1968).

15. Der, J., A Study of General Three Dimensional Boundary Layer Problems by an Exact Numerical Method, AIAA J., Vol 9, No. 7, 1294-1302 (1971).

16. Hall, M. G., A Numerical Method for Calculating Steady Three Dimensional Laminar Boundary Layers, R.A.E. Tech. Report 67145, June 1967.

17. Crank, J. and Nicolson, P., A Practical Method for Numerical Evaluation of Solution of Partial Differential Equations of the Heat Conduction Type, Proc. Camb. Phil Soc. Vol. 43, p 50 (1947).

18. Lew, H. G., Investigation of the Ignition and Burning of Materials in Space Cabin Atmospheres, NASA CR 128068 (1972).

19. MacCormack, R. W., The Effect of Viscosity in Hypervelocity Impact Cratering, AIAA 7th Aerospace Sciences Mtg., Paper No. 69-354 (1969).

20. Bortner, M., private communication.

21. Bortner, M., "A Review of Data Constants of Selected Reactions of Interest in Re-entry Flow Fields in the Atmosphere", National Bureau of Standards Technical Note 484, May 1969.

22. Bortner, M. (ed.), DASA Reaction Rate Handbook, Defense Atomic Support Agency Information and Analysis Center, October, 1967.

23. Browne, W. G., "Thermodynamic Properties of Some Atoms and
    Atomic Ions", "Thermodynamic Properties of Some Diatoms and
    Diatomic Ions at High Temperatures", and "Comparison of
    Thermal Functions Generated for Species in the High Temperature
    Air System with Literature Values", GE-RS, Physics TM No. 2, 8,
    and 10, 1962.

24. Yun, K. S., and Mason, E. A., "Collision Integrals for the
    Transport Properties of Dissociating Air at High Temperatures",
    Physics of Fluids, Vol. 5, No. 2, 155-164, Feb. 1962.

25. Lew, H. G., Nonequilibrium Blunt Body Flow with Material Ablation
    Including Transverse Curvature and Merged Viscous Effects at
    Stagnation Regions GE TIS Doc. No. 69SD760, SAMSO TR 69-292 (1969).

VIII. TABLE

Chemical System of Air Reactions and Rates

TABLE

CHEMICAL SYSTEM OF AIR REACTIONS AND RATES

REACTIONS	FORWARD			BACKWARD		
	a	b	c	a	b	c
1. $O_2 + M_1 = 2O + M_1$	8.74 (17)	-1	.594 (5)	7.26 (14)	- .5	0
2. $N_2 + M_2 = 2N + M_2$	2.41 (18)	- .8	.1132 (6)	1.34 (17)	- .8	0
3. $NO + M_3 = O + N + M_3$	1.45 (16)	0	.754 (5)	3.63 (15)	0	0
4. $O + NO = N + O_2$	4.33 (7)	1.5	.181 (5)	1.81 (8)	1.5	.3 (4)
5. $O + N_2 = N + NO$	6.02 (12)	0	.38 (5)	1.32 (13)	0	0
6. $O + N = NO^+ + e$	5.18 (11)	0	.319 (5)	1.44 (21)	-1.5	0
7. $N + N = N_2^+ + e$	4.7 (8)	1.3	.678 (5)	5.3 (17)	- .2	0
8. $O + O = O_2^+ + e$	6.62 (7)	1.3	.807 (5)	7.22 (18)	- .7	0
9. $N + M = N^+ + e + M$	1.81 (19)	-1.	.169 (6)	1.09 (27)	-2.5	0
10. $O + M = O^+ + e + M$	3.01 (18)	-1.	.158 (6)	7.25 (26)	-2.5	0
11. $N_2 + M = N_2^+ + e + M$	1.81 (4)	2	.181 (6)	1.09 (12)	.5	0
12. $O_2 + M = O_2^+ + e + M$	6.02 (3)	1.5	.14 (6)	5.8 (11)	0	0
13. $NO + M = NO^+ + e + M$	6.02 (17)	-1.	.1079 (6)	3.63 (26)	-2.5	0
14. $N_2^+ + O_2 = N_2 + O_2^+$	1.20 (14)	0	0	3.61 (13)	0	.409 (5)
15. $N_2^+ + O = NO^+ + N$	1.51 (14)	0	0	2.71 (14)	0	.354 (5)

CHEMICAL SYSTEM OF AIR REACTIONS AND RATES   (Continued)

REACTIONS	FORWARD			BACKWARD		
	a	b	c	a	b	c
16. $N^+ + O_2 = NO^+ + O$	3.01 (14)	0	0	6.02 (12)	.5	.872 (5)
17. $N^+ + NO = N + NO^+$	4.82 (14)	0	0	2.11 (14)	.5	.492 (5)
18. $O^+ + N_2 = NO^+ + N$	6.02 (11)	0	0	1.81 (11)	0	.124 (5)
19. $O^+ + O_2 = O + O_2$	1.2 (13)	0	0	1.81 (12)	0	.179 (5)
20. $O_2^+ + NO = O_2 + NO^+$	4.82 (14)	0	0	2.53 (14)	0	.322 (5)

$k = aT^b \exp(-c/T)$, moles, sec, $^{\circ}K$, cm

$N(x) = N^x$

TABLE

CHEMICAL SYSTEM OF AIR REACTIONS AND RATES   (Continued)

Third Body Efficiencies

Species	M_1	M_2	M_3	M_4
O_2	25	1	1.1	1
N_2	25	3.24	1.1	1
O	105	1	50	1
N	1	21.6	50	1
NO	1	1	50	1

IX. <u>List of Figures</u>

FIGURE 1.1   SCHEMATIC THREE DIMENSIONAL BOUNDARY LAYER DEVELOPMENT
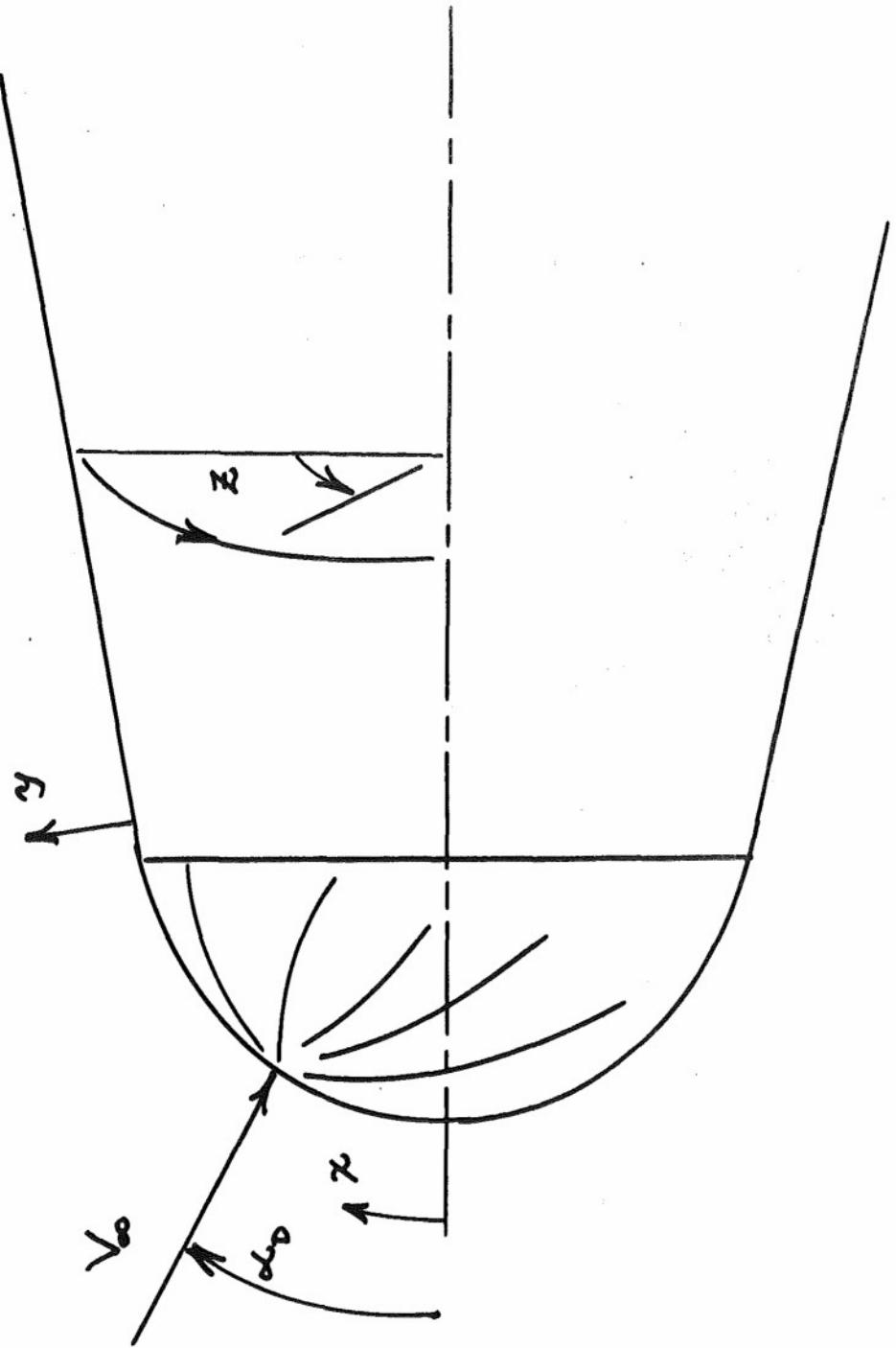
FIGURE 2.1 COORDINATE SYSTEM
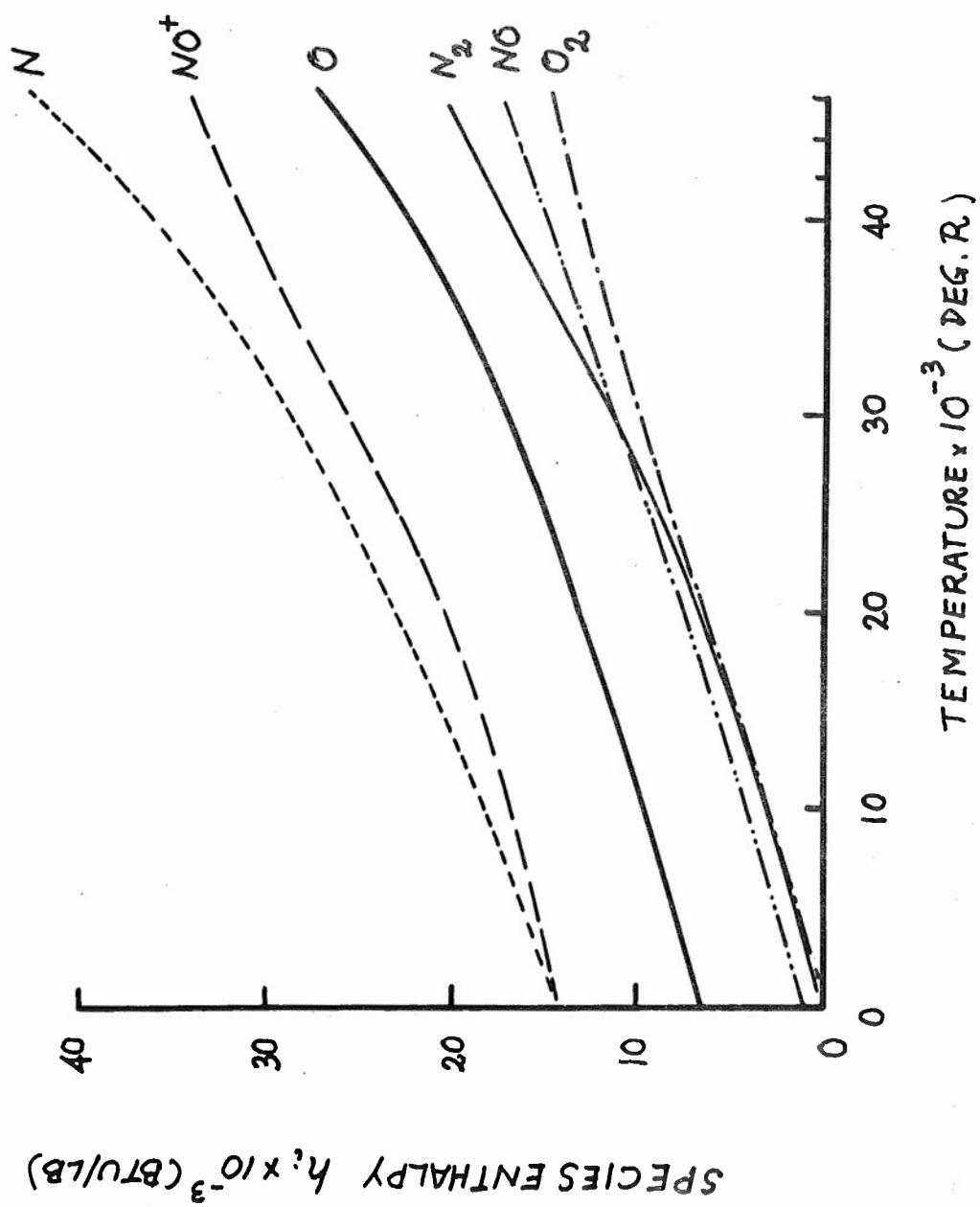
FIGURE 4.1   SPECIES ENTHALPY

- 45 -
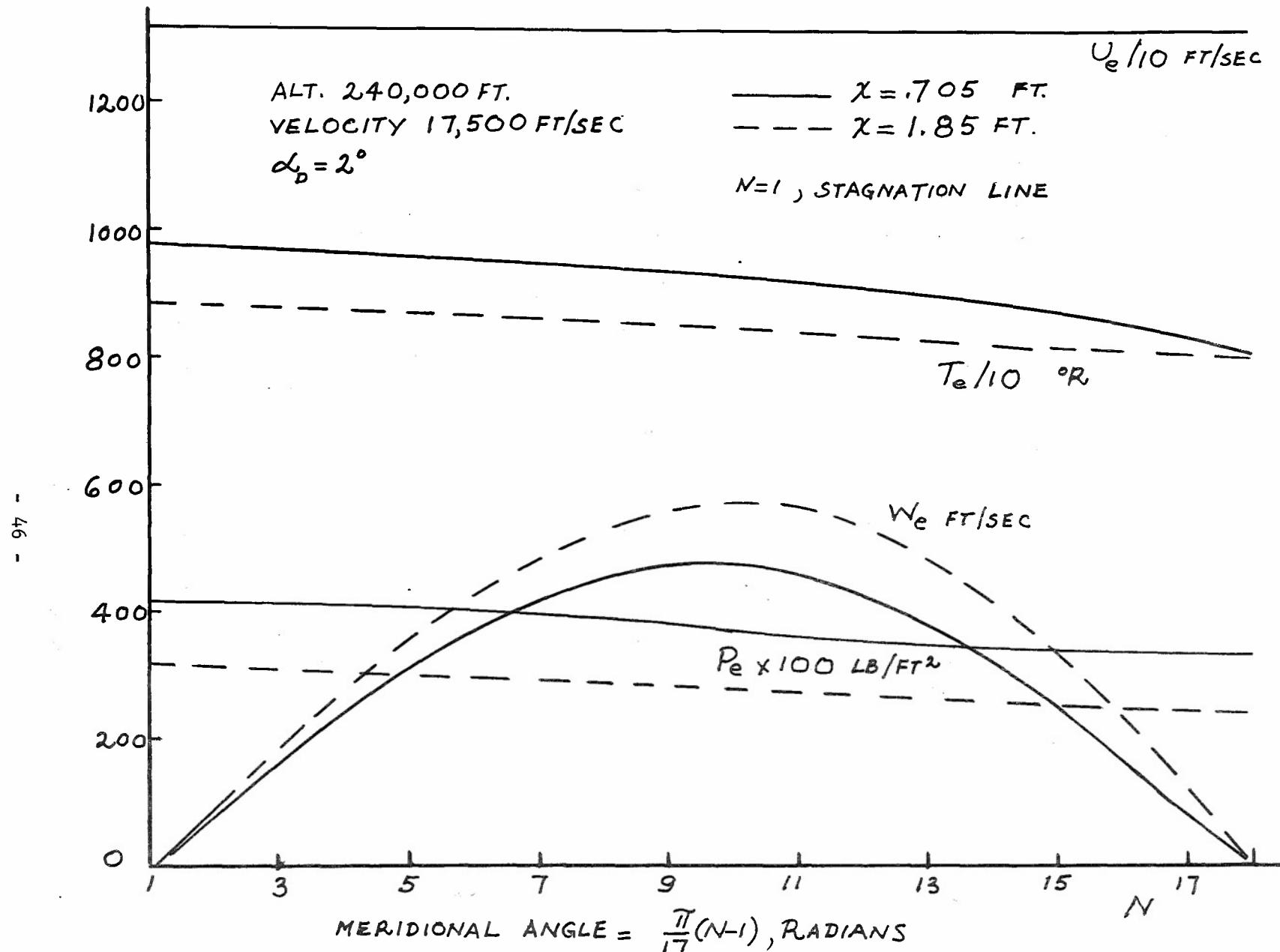
FIGURE 5.1   AZIMUTHAL DISTRIBUTION OF INVISCID VELOCITY COMPONENTS, TEMPERATURE AND PRESSURE
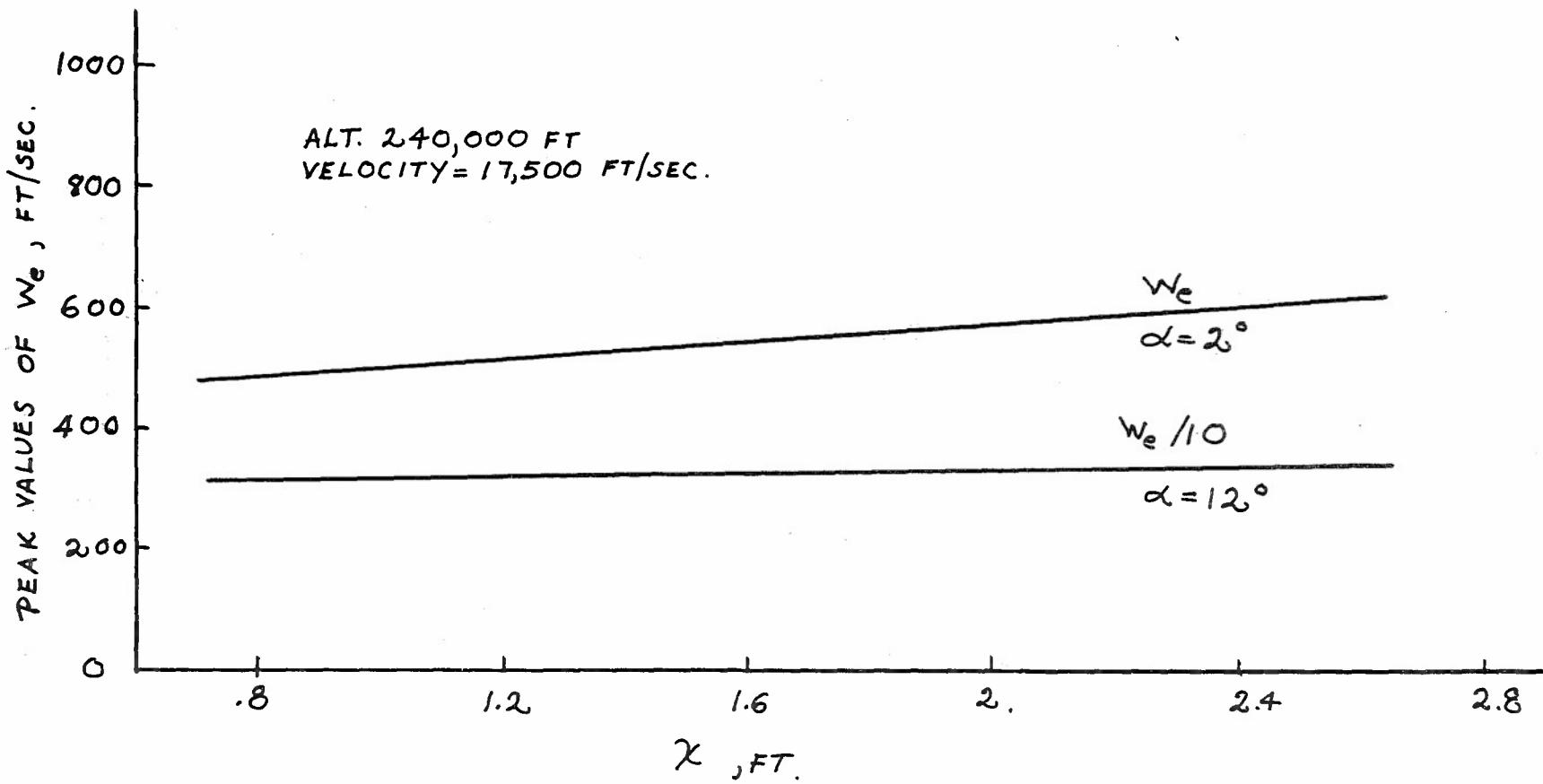
FIGURE 5.2 DISTRIBUTION OF VELOCITY w_e

$x = 2.4$ FT   ALT. 240,000 FT.

$\alpha_D = 12°$ VELOCITY 17,500 FT/SEC.

N=1 , STAGNATION LINE

MASS FRACTION

.10

.08

.07

.06

.05

5   9   13   17

N

MERIDIONAL ANGLE $= \frac{\pi}{17}(N-1)$, RADIANS
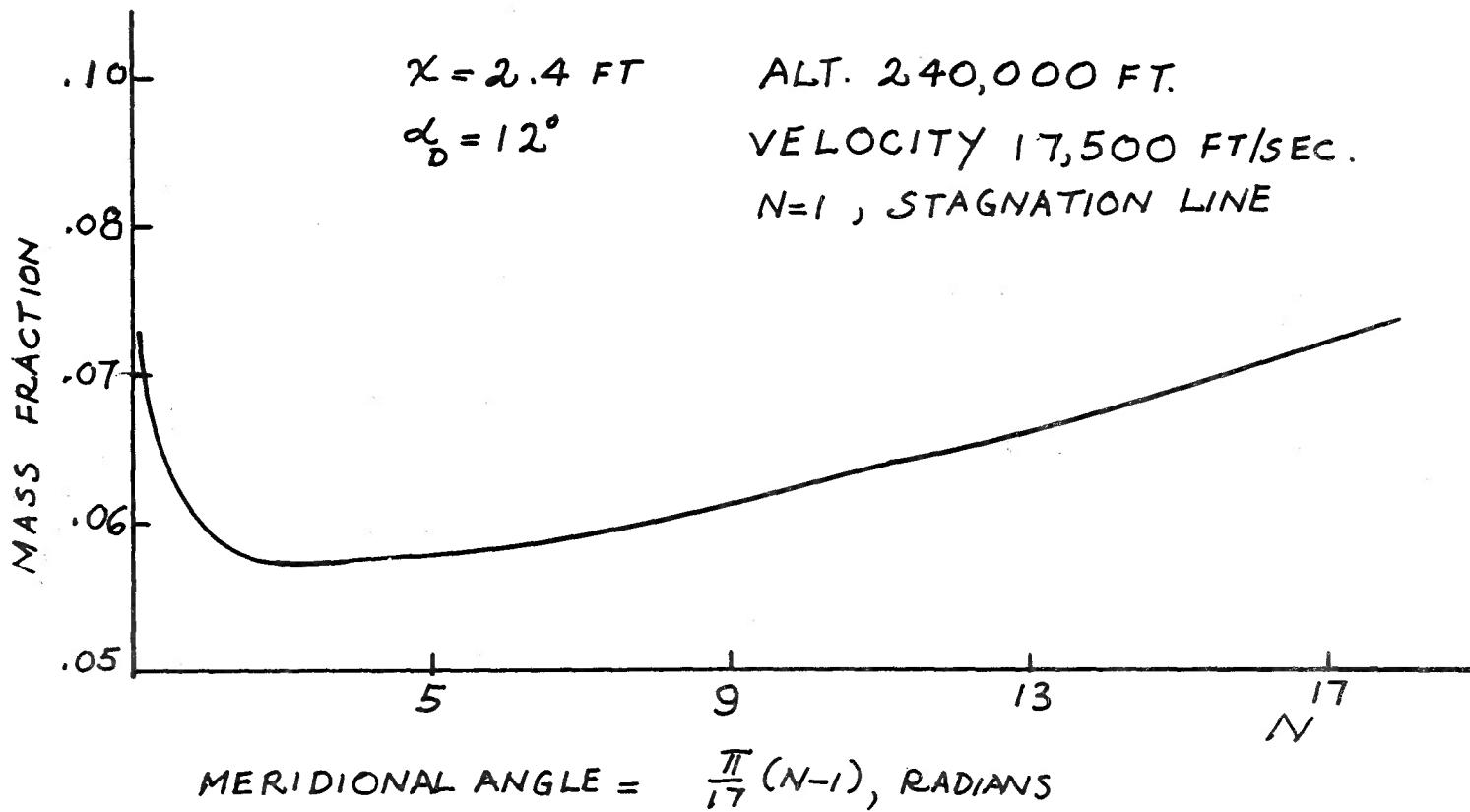
FIGURE 5.3   AZIMUTHAL DISTRIBUTION OF ATOMIC OXYGEN AT THE BOUNDARY LAYER EDGE
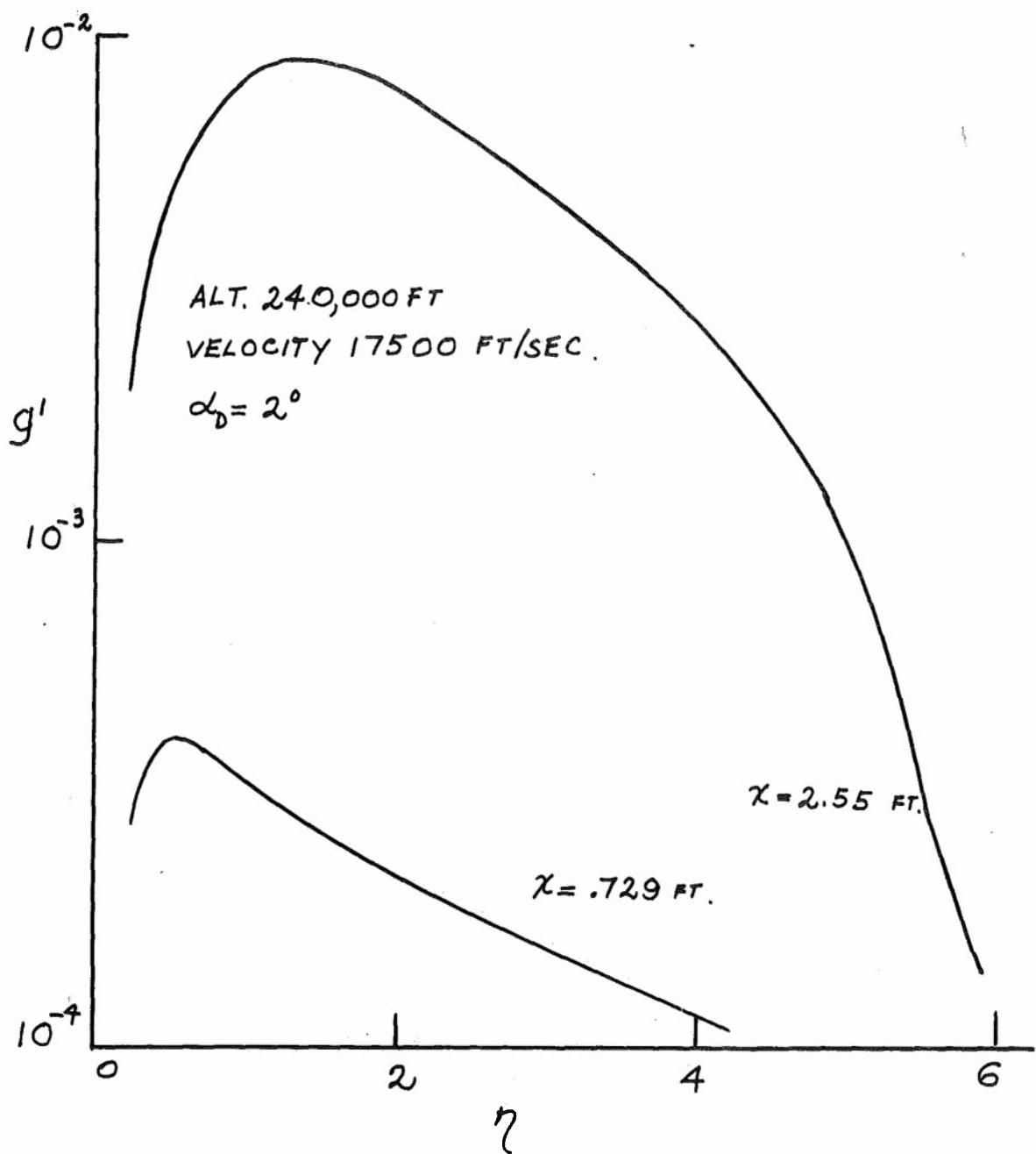
FIGURE 5.4 VARIATION OF ANGULAR VELOCITY GRADIENT AT THE
WINDWARD STAGNATION LINE
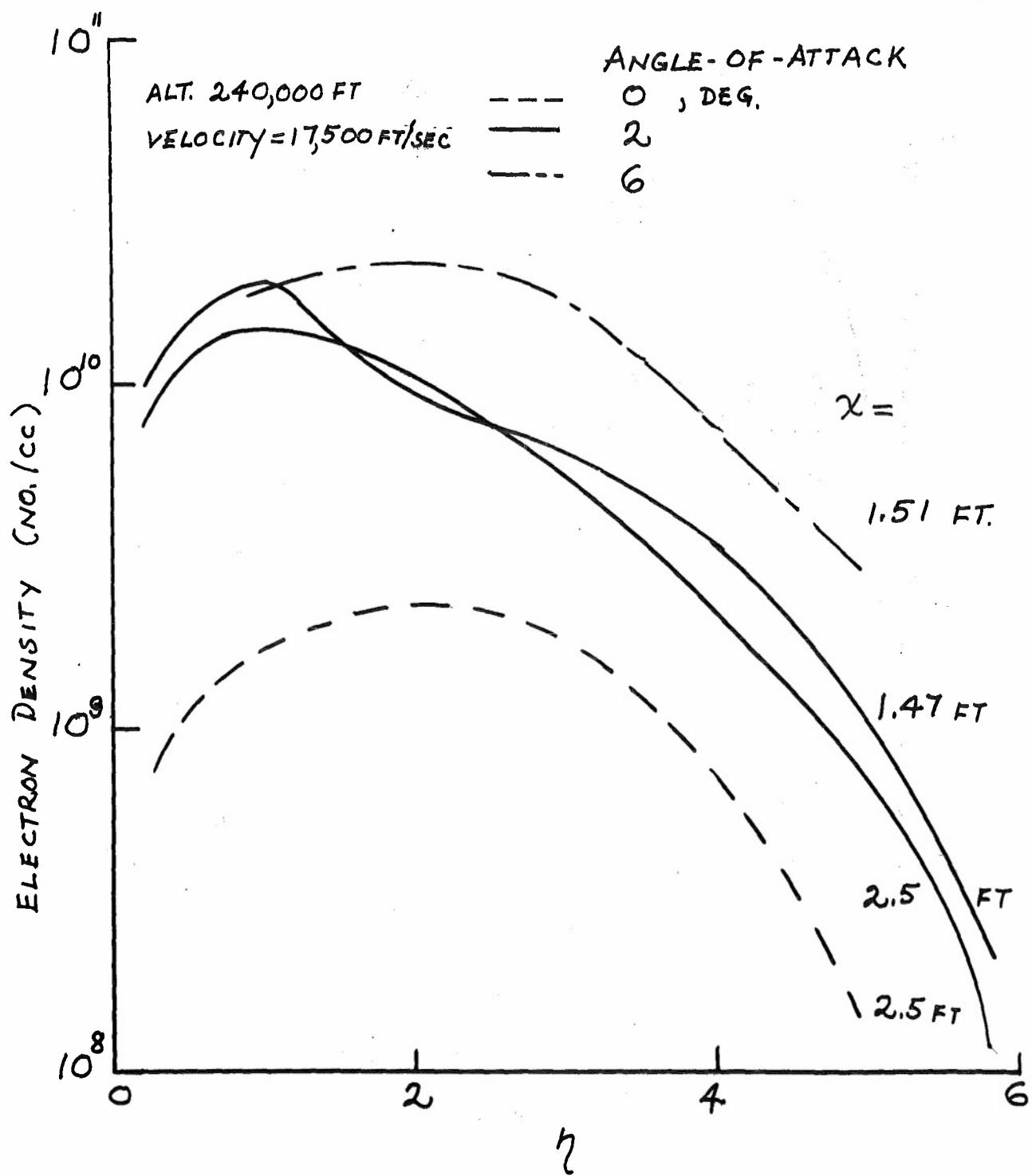
FIGURE 5.5 ELECTRON DENSITY DISTRIBUTION AT THE WINDWARD STAGNATION
LINE FOR ANGLE-OF-ATTACK